Texture vs morphology in ZnO nano-rods: On the x-ray diffraction characterization of electrochemically grown samples

D. Ariosa, F. Elhordoy, E. A. Dalchiele, R. E. Marotti, and C. Stari

Citation: J. Appl. Phys. **110**, 124901 (2011); doi: 10.1063/1.3669026
View online: http://dx.doi.org/10.1063/1.3669026
View Table of Contents: http://jap.aip.org/resource/1/JAPIAU/v110/i12
Published by the American Institute of Physics.

Texture vs morphology in ZnO nano-rods: On the x-ray diffraction characterization of electrochemically grown samples

D. Ariosa,[1,2,a)] F. Elhordoy,[1] E. A. Dalchiele,[1] R. E. Marotti,[1] and C. Stari[1]
[1]*Instituto de Física & CINQUIFIMA Facultad de Ingeniería, Universidad de la República, Herrera y Reissig 565, C.C. 30, 11000 Montevideo, Uruguay*
[2]*IPMC, Institute of Physics of Condensed Matter, IPMC/FSB/EPFL, Lausanne, Switzerland*

(Received 26 April 2011; accepted 14 November 2011; published online 19 December 2011)

Texture characterization in thin films from standard powder x-ray diffraction (XRD) rely on the comparison between observed peak relative intensities with those of powder diffraction standards of the same compound, trough the so-called texture coefficient (TC). While these methods apply for polycrystalline materials with isotropic grains, they are less accurate—and even wrong—for anisotropic materials like ZnO oriented single-crystal nano-rods, which would require the use of dedicated XRD texture setups. By using simple geometrical considerations, we succeed in discriminating between texture and morphology contributions to the observed intensity ratios in powder diffraction patterns. On this basis, we developed a method that provides a quantitative determination of both texture (polar distribution) and morphology (aspect ratio of nano-rods), using simple x-ray powder diffraction. The method is illustrated on a typical sample from a series of Zinc oxide (ZnO) nano-rod arrays grown onto a gold thin film sputtered onto a F:SnO_2-coated glass substrate (FTO) by using cathodic electro-deposition. In order to check the consistency of our method, we confronted our findings with scanning electron microscope (SEM) images, grazing incidence diffraction (GID), and XRD pole-figures of the same sample. Nevertheless, the proposed method is self-consistent and only requires the use of a standard powder diffractometer, nowadays available in most solid-state laboratories. © *2011 American Institute of Physics*.
[doi:10.1063/1.3669026]

I. INTRODUCTION

Among the wide range of properties of Zinc oxide (ZnO) in the fields of optoelectronics and sensor devices, one-dimensional ZnO nanostructures, specifically ZnO nano-rods (ZNRs),[1,2] have great potential applications. Cathodic electro-deposition[3–5] is, after chemical bath deposition,[1,6] the most suitable and cheapest method to grow large-scale devices for commercial applications. On another hand, the use of one-dimensional nanostructured materials for applications requires a good control of phase purity, crystalline morphology, and crystallographic alignment through the preparation process. The issues of nano-rod morphology and alignment are crucial in determining the internal quantum efficiency of dye-sensitized solar cells, as explicitly discussed in reference.[2] X-ray powder diffraction (XRD) is the appropriate tool to control chemical phase purity, while direct space scanning electron microscope (SEM) images and XRD pole figures are usually employed, respectively, to characterize morphology and texture. However, standard x-ray powder diffraction is widely used, not only to control phase purity but also for texture characterization, e.g., Refs. 7–9. In this kind of approach, texture characterization is achieved by comparing observed peak relative intensities with those of powder diffraction standards of the same compound, trough the so-called texture coefficient (TC), proposed by C. Barret and T. B. Massalski[10] after the work of G. B. Harris (1952).[11] As we shall see in the following, this method is unable to discriminate between real texture and morphology contributions. An alternative approach, developed by M. D. Vaudin *et al.*,[12] consists in correcting the rocking-curve (RC) from absorption and defocusing in order to obtain the actual angular distribution for the preferred orientation. However, this method requires the use of a diffractometer in which one can decouple θ and 2θ angles and, as for the TC approach, it does not separate texture from morphology. In the present contribution, we discuss the applicability of the TC method[10] for polycrystalline samples formed of highly anisotropic crystallites (nanorods) with a given crystallographic orientation along their longer axis. After noticing, the strong contribution of the crystallites' shape on the relative Bragg peak intensities, we work out an adapted method in order to include the grain morphology into the texture analysis starting with the same idea of Ref. 10, i.e., comparing the observed diffraction relative intensities with those of a standard (isotropic) powder sample of the same compound. For practical reasons, we center the discussion on a typical sample from a series of ZNRs arrays grown onto F:SnO_2 coated substrates by using cathodic electro-deposition. We also confront our results with those extracted from direct space SEM images, grazing incidence diffraction (GID), and pole figures, in order to support the discussion and as a consistency check for the approach. This method, which just needs the use of a standard powder diffractometer, can be generalized to all kind of samples within the class of one-dimensional oriented nanostructures.

a)Electronic mail: dariosa@fing.edu.uy.

II. EXPERIMENTAL

A. Sample fabrication

ZnO nano-rod arrays were grown by the electrochemical deposition method from a 1 mM zinc acetate aqueous solution maintained at 70 C. For supporting electrolyte, 0.1 M sodium acetate was employed to ensure a good electrical conductivity in the aqueous solution (Milli-Q quality water, 18 M cm). The pH of the solution was initially adjusted to 6.76. The ZnO nano-rod were grown onto a gold thin film (1500 Å) sputtered onto a F:SnO_2-coated glass substrates (fluorine-doped tin oxide, or FTO), 10 Ω/□ sheet resistance. The electrodeposition was performed in a conventional three-electrode electrochemical cell with the substrate as the cathode, a zinc sheet as the counter electrode and a saturated calomel electrode (SCE) as the reference one. Electrodeposition was carried out potentiostatically at −1.0 V vs. SCE. The electrolyte was saturated with pure molecular oxygen by bubbling for 45 min prior to start the electrodeposition and continuously during of the growth process. The electrochemical deposition time was 3600 s. After electrodeposition, ZnO nano-rods/Au/FTO were thoroughly and carefully rinsed with DI water to remove un-reacted products from the surface and dried under a moderate air flux.

B. Structural characterization

Standard $\theta - 2\theta$ scans were performed on a Philips PW1840 diffractometer (30 kV, 40 mA, Cu Kα radiation with $\lambda = 1.5406$ Å). The diffraction peaks from ZnO and SnO_2 have been indexed by reference to the JCPDS powder diffraction files.[13] GID and pole figures were obtained, with the same radiation source, on a Philips X'Pert multiple-purpose diffraction (MRD) goniometer.

Due to practical reasons, diffraction intensities in the present work are taken as the height of the peaks instead of the, in principle, more adequate integrated intensities. Indeed, integrated intensity (total diffracted energy) is an intrinsic quantity of the sample, while peak heights are much more sensitive to instrumental details. In addition, as we shall see in the Sec. III, for small grains, peak broadening starts to be important. However, the determination of the integral intensity of a given peak needs, in addition to the background subtraction, the subtraction of the neighboring peaks contribution. In order to be reliable, these operations need high signal/noise ratios, which in turn need longer acquisition times for the diffraction pattern. In our everyday practice, we have realized that the long acquisition times (>3 h) and, in addition, the considerable time required for data analysis using integrated intensities does not lead to a significant improvement of the results, compared with the peak height strategy from which we obtain similar results in less than 40 min. It is important to enphasize here that the main goal of the present contribution is to provide with an easy and rapid feedback between XRD characterization and cathodic electro-deposition, and thus, within this context, the choice of the peak height strategy is considered to be adequate.

Scanning electron microscopy (SEM) pictures were obtained on a JEOL JSM/5900 LV SEM equipment at an acceleration voltage of 20 kV.

III. RESULTS AND DISCUSSION

A standard $\theta - 2\theta$ XRD scan in Bragg-Brentano (BB) geometry on a nano-rod array of ZnO grown onto a polycrystalline F:SnO_2 film is shown in Figure 1(a). Bragg peak positions are indicated by a full black circle (•) for ZnO and by an empty square (□) for F:SnO_2; Au (200) reflection is indicated by an asterisk (*). ZnO has an hexagonal structure with crystallographic parameters: a = 3.249 Å; c = 5.205 Å; $\alpha = \beta = 90°$; $\gamma = 120°$. ZnO peaks show high intensities relative to the background, denoting a good crystallinity of the sample. The absence of other peaks denotes the purity of the grown phase. At a first glance, one notices the high relative intensity of the (002) reflection at 34.4°, compared with the one expected from a powder standard. Indeed, for a powder sample the ratio (I_{002}/I_{101}) is about 0.56, while the observed specimen shows a ratio of 3.64, i.e., more than 6 times larger. This would suggest a strong preferential alignment of the [001] direction along the normal to the sample surface. In order to obtain a semi-quantitative estimation of the texture, one usually calculates the TC, defined by[10,11]

$$TC_{(xyz)} = \frac{I_{xyz}/I^0_{xyz}}{\frac{1}{N}\sum I_{hkl}/I^0_{hkl}}. \quad (1)$$

In expression (1), I_{hkl} are the observed peak relative intensities, I^0_{hkl} the relative intensities for the isotropic random oriented powder and N the number of considered Bragg reflections over which the sum in the denominator is carried on. By construction, the TC ranges from 1 (no texture) to N (single oriented crystals). In the case of the (002) peak, taking up to 16 reflections in Figure 1(a) for the sum, we obtain $TC_{002} = 3.1$, which is a clear indication for texture.

In Figure 1(b), we show a comparison between a BB scan (light curve) and a GID scan (dark curve). These scans have been performed on the Philips X'Pert MRD goniometer, which allows to decouple the motions of the detector (2θ-axis) and the sample (Ω-axis). With this particular instrument dedicated to texture analysis, the divergence of the primary beam together with the geometry of the secondary optics, one obtains a much lower resolution than with the standard powder diffractometer and an additional angular dependent intensity modulation. A superposition of both scans around the ZnO (002) reflexion is shown in the enlargement on the top right corner. Curiously, when examining the GID, taken with a fixed 4° incidence angle (dark curve in Figure 1(b), the ZnO relative intensities look very similar to the ones of the BB scan, still dominated by the ZnO (002) peak. In the case of a clear (002) texture, one would expect a strong reduction of the (002) peak intensity in the GID. But the only change we observe is a global reduction in the SnO_2 peak intensities, which is to be expected in grazing incidence for a hidden layer. This puzzling behavior points out the need of an alternative explanation, beyond texture, for the observed relative intensities modification in ZnO. As illustrated in the SEM pictures of Figure 2, we are dealing with single crystalline c-axis oriented nano-rods. Thus, we can guess that grain morphology is playing here an important role. Diffraction theory[14] establishes that the intensity of a

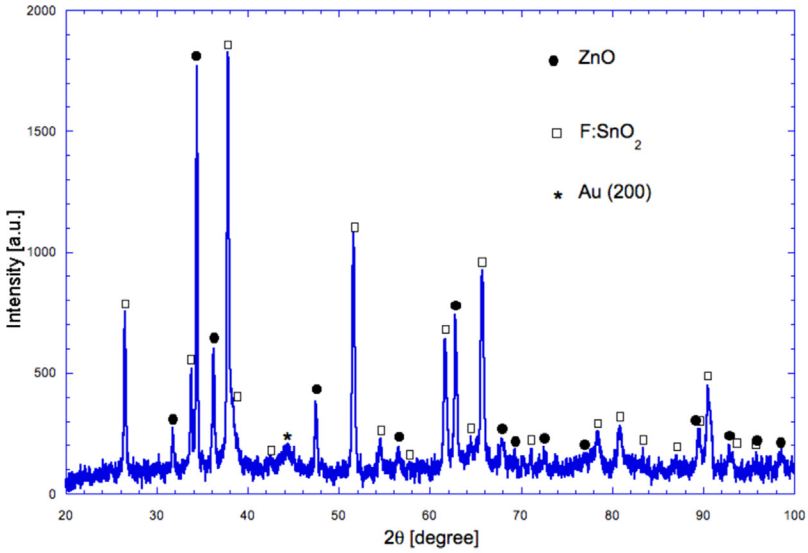

(a)

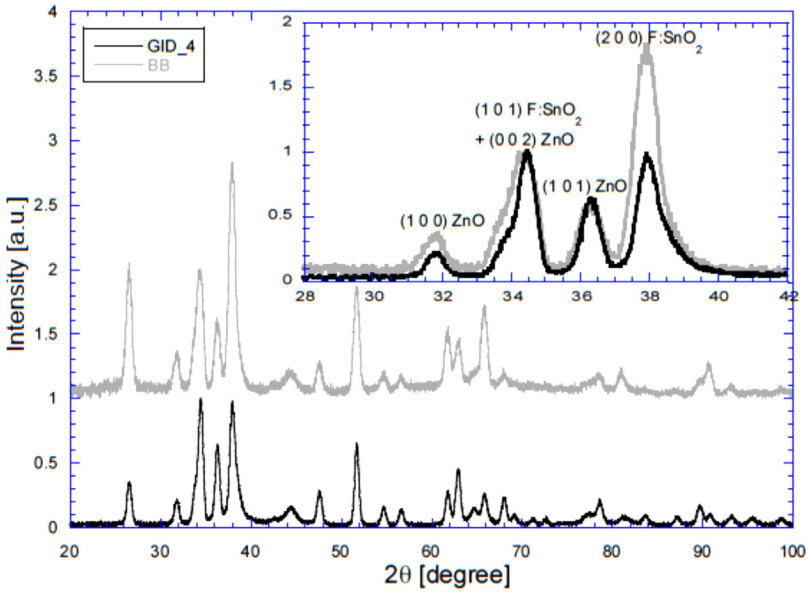

(b)

FIG. 1. (Color online) (a) Bragg-Brentano XRD spectra of ZnO nano-rods grown by electrochemical method onto a polycrystalline F:SnO_2 film. Bragg peak positions are indicated by a full black circle (•) for ZnO and by an empty square (□) for F:SnO_2. Au (200) reflection is indicated by an asterisk (*). (b) Comparison between Bragg-Brentano (gray curve) and Grazing-incidence (dark curve) XRD spectra of ZnO nano-rods. The inset shows an enlargement of the superposition of both scans around the ZnO (002) reflexion.

given Bragg reflection in a randomly oriented homogeneous powder depends upon multiple factors; essentially: incoming beam intensity, unit cell structure factor, multiplicity, Lorentz-polarization factor, and grain size along the bisecting direction between incident and diffracted beams, i.e., the surface normal in BB geometry. Among all the preceding factors, the sole difference between a standard ZnO powder and ZnO nano-rods is, beyond texture, the anisotropic grain size of the crystallites which induces intensity and peak broadening variations depending on the nano-rod tilting angle ψ with respect to the surface normal. Indeed, in the case of nano-rods, we have to consider the effective size l along the surface normal, determining the number of planes that contributes to the diffraction in this direction. This effective size l is the projection of the nano-rod long-axis L on the surface normal direction bounded, at high inclination angles ($\psi > \psi^* = \tan^{-1}(L/d)$), by the section diameter d:

$$l = L\max[\cos\psi, r\sin\psi]; \quad r \equiv \frac{d}{L}. \tag{2}$$

Since the diffracted intensity scales with the square of this length, the shape related correction factor for the intensity reads

$$f_{corr} = \max[\cos^2\psi, r^2\sin^2\psi], \tag{3}$$

where r is the aspect ratio of the nano-rod. In the case of c-axis oriented nano-rods, the correction factor in Eq. (3) is maximal for (00l) reflections and minimal for (hk0) ones. For isotropic grains, i.e., spherical shape, the cylindrical model of Eq. (2) no longer applies and the correction is trivially 1 for all peaks. According to Eq. (3), the intensity correction for the (002) peak is 1, while for the intensity of the (101), which appears when the c-axis oriented nano-rod is tilted by $\psi_{101} = 61.6°$, is 0.227. Thus, even for randomly oriented

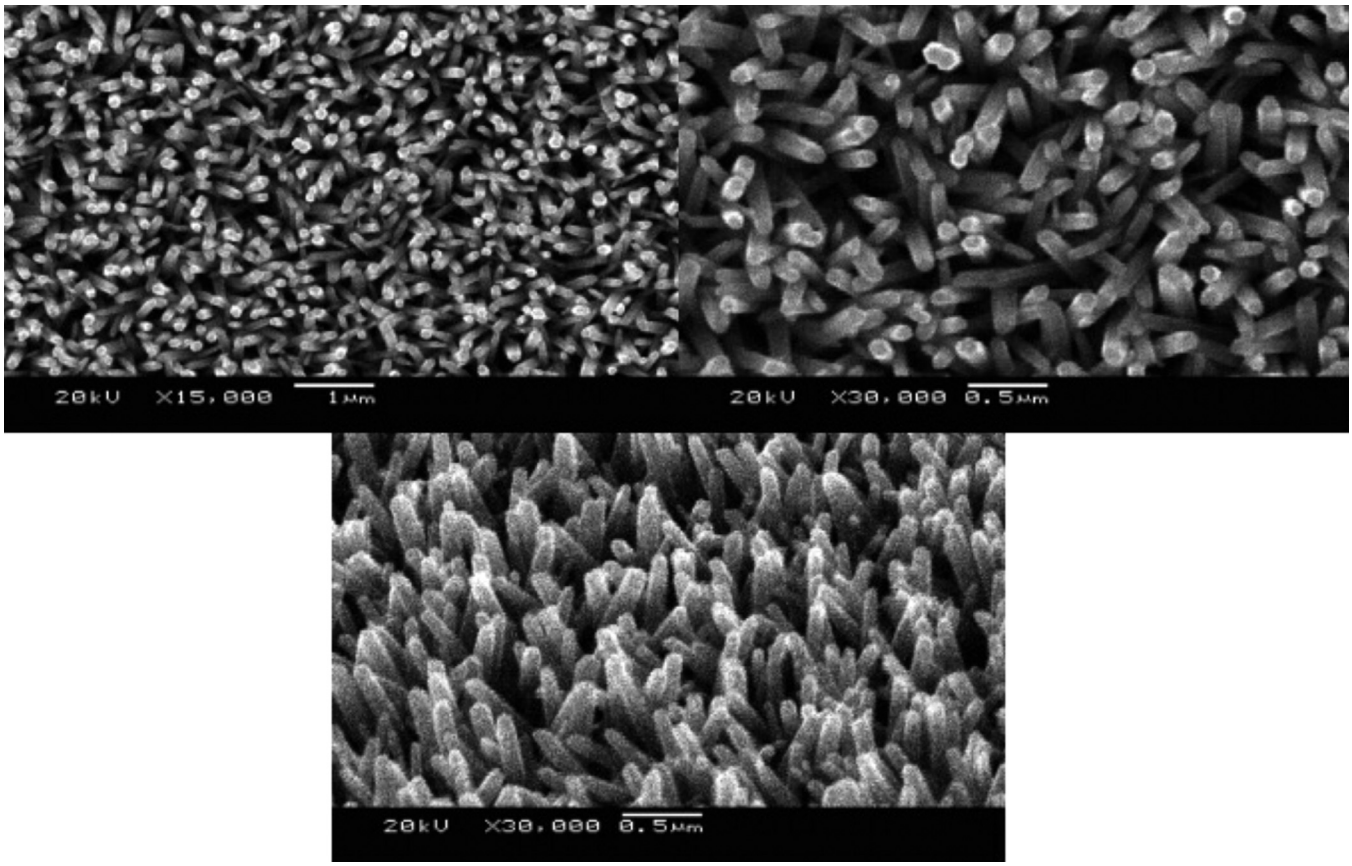

FIG. 2. SEM images of ZnO nano-rods of the same sample as in Figure 1: (a) top picture × 15 000 magnification; (b) top picture × 30 000 magnification; (c) 60° side view × 30 000 magnification.

nano-rods, the intensity ratio I_{002}/I_{101} would be increased from 0.56 in a powdered sample, to 2.475 in randomly oriented nano-rods. A considerable amount of the observed anomalous intensity ratio (3.64) can thus be assigned to the elongated morphology and not only to the texture.

Let us calculate, from the 16 calculated shape-correction factors in Table I, the corresponding TC for randomly oriented nano-rods for an aspect ratio $r = 1{:}5$, according to Eq. (1): $TC_{(002)} = 16/\sum f_{corr} = 2.623$. The result is again close the texture coefficient ($TC = 3.1$) directly estimated from the data in Figure 1 and far from unity, showing the importance of the morphology contribution to the usual TC and implying the overestimation of the actual texture. In fact, SEM pictures in Figure 2 show a broad angular distribution in contrast with the relatively high TC ($TC_{(002)} = 3.1$) previously estimated from Eq. (1).

The angular distribution can be directly measured by means of a pole figure as shown in Figure 3. For a (001) texture, the (002) Bragg reflection is expected to be centered at $\psi = 0$, as observed in Figure 3(a), and the maximum of the (101) reflection is expected at an inclination angle $\psi = 61.6°$, as confirmed in Figure 3(b). Thus, pole figures confirm both, the (001) preferred orientation, and the weakness of the texture: the full width at half maximum (FWHM) of the polar distribution in Figure 3(a) is about 120°. In addition, one notices the in-plane isotropy of the pole figure,[15] indicating the absence of in-plane preferred orientation.

At this point, it is instructive to apply the same analysis as above to the underlying $F{:}SnO_2$, which has a tetragonal structure with crystallographic parameters: $a = 4.738$ Å; $c = 3.188$ Å; $\alpha = \beta = \gamma = 90°$. The situation for the bottom $F{:}SnO_2$ layer is quite different: commercial FTO film substrates are known to be made of isotropic grains and present

TABLE I. Calculated shape correction factors for randomly oriented nano-rods with aspect ratio r = 1:5. Columns from left to right: Miller indices, Bragg angles, polar tilt angles, tabulated powder intensity ratios, calculated shape-correction factors following Eq. (3) and observed correction factors.

ZnO (hkl)	2θ (°)	ψ (°)	I_{hkl}/I_{101} [%] (tab.)	f_{corr}^{shape} (calc.)	f_{corr} (exp.)
(100)	31.777	90	71	0.04	0.067
(002)	34.433	0	56	1.00	1.000
(101)	36.264	61.605	100	0.23	0.154
(102)	47.554	42.767	29	0.54	0.318
(110)	56.611	90	40	0.04	0.064
(103)	62.879	31.659	35	0.72	0.545
(200)	66.396	90	6	0.04	0.000
(112)	67.970	58.027	28	0.28	0.122
(201)	69.108	74.875	14	0.07	0.090
(004)	72.594	0	3	1.00	1.016
(202)	76.985	61.605	5	0.23	0.388
(104)	81.417	24.819	3	0.82	0.401
(203)	89.646	50.962	10	0.40	0.421
(210)	92.824	90	4	0.04	0.000
(211)	95.340	78.452	10	0.04	0.109
(114)	98.658	38.695	5	0.61	0.494

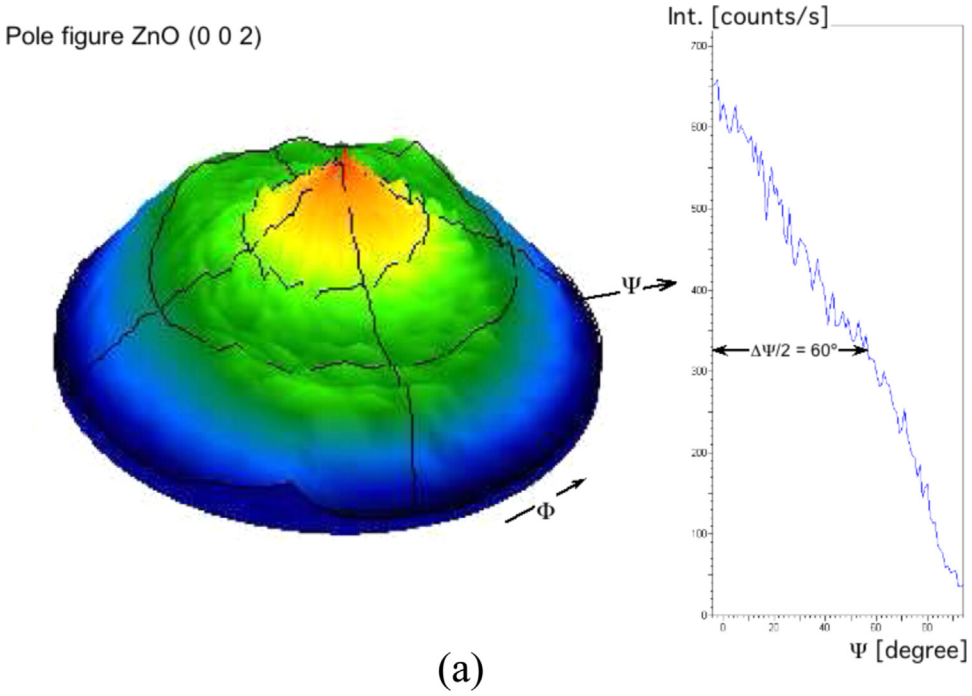

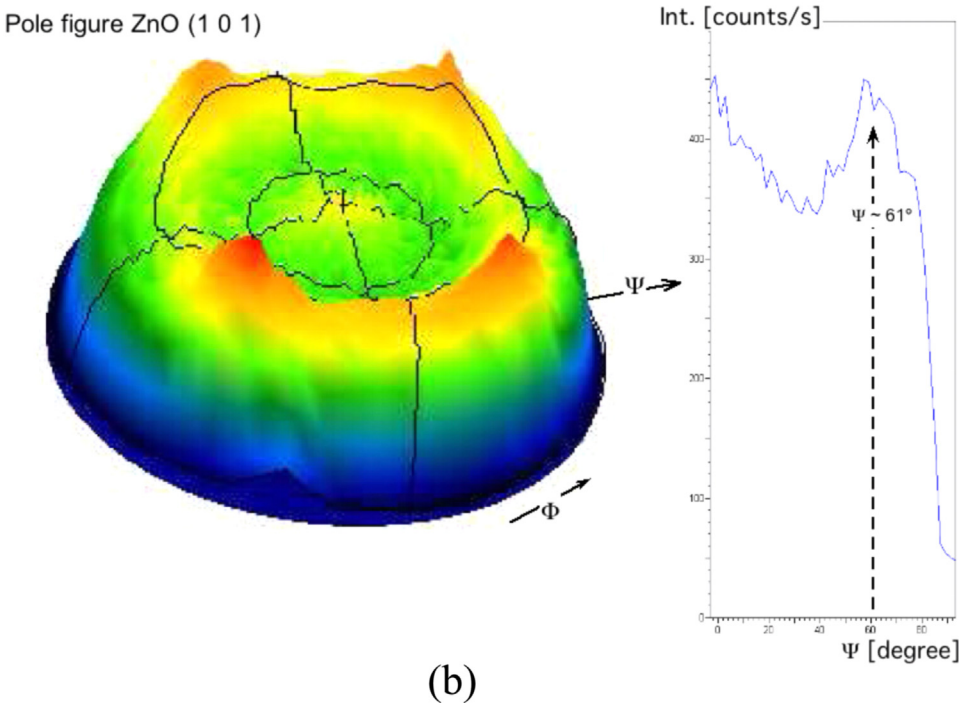

FIG. 3. (Color online) ZnO pole figures (002) in (a) and (101) in (b). 3D plot (left hand panel) and ψ scan (right hand panel).

a slight texture along the (tetragonal) [100] direction. From the experimental relative peak intensities of the F:SnO_2 contribution in Figure 1, according to Eq. (1), we extracted TC = 2.9, estimated from the intensity values of 19 peaks (column 5 in Table II). This TC value corresponds to the expected texture but we cannot exclude, a priori, an eventual shape contribution. In order to check this point, we can evaluate the eventual morphology contribution to the TC, assuming a moderate aspect ratio $r < 1$: 2. According to Eq. (3), taking the inclination angles in Table II, we found TC(002) = 1.75. This value is only 60% of the measured TC value but, again, it is not a proof that the intensity variations are due merely to the polar distribution. The only way to directly prove the angular distribution is the pole figure or the Psi-scan. We then performed a pole figure measurement for (200) and (110) SnO_2 reflections (the peaks appearing at Bragg angles about 37.9° and 26.5° in Figure 1, as shown in Figure 4. As one can immediately see, the FWHM of the polar distribution of the [200] direction in Figure 4(a) is about 60°, indicating for the bottom F:SnO_2 layer a much better texture than for the ZnO upper layer, even if their relative TC values seem to indicate the opposite. The maximum for

TABLE II. Calculated shape and texture correction factors for the F:SnO_2 underlying layer. For the grain shape it is assumed an aspect ratio r < 1:2. Columns from left to right: Miller indices, Bragg angles, polar tilt angles, tabulated powder intensity ratios, observed intensity ratios, calculated shape-correction factors and calculated Gaussian texture-correction factors.

F:SnO_2 (hkl)	2θ (°)	ψ (°)	I_{hkl}/I_{110} [%] (tab.)	I_{hkl}/I_{200} [%] (exp.)	f_{corr}^{shapte} (calc.)	f_{corr}^{text} (calc.)
(110)	26.585	45	100	42	0.50	0.21
(101)	33.863	56.065	80	23	0.31	0.09
(200)	37.950	0	25	100	1.00	1.00
(111)	38.967	60.827	6	3	0.24	0.06
(210)	42.635	26.565	2	5	0.80	0.58
(211)	51.763	41.849	65	65	0.55	0.26
(220)	54.754	45	18	7	0.50	0.21
(002)	57.796	90	8	4	0.25	0.00
(310)	61.877	18.435	14	36	0.90	0.77
(112)	64.709	72.314	18	4	0.23	0.02
(301)	65.955	26.354	16	52	0.80	0.59
(202)	71.247	56.065	8	6	0.31	0.09
(321)	78.697	39.712	12	8	0.59	0.30
(400)	81.131	0	4	10	1.00	1.00
(222)	83.683	60.827	8	4	0.24	0.06
(330)	87.223	45	4	3	0.50	0.21
(312)	89.754	46.271	8	9	048	0.19
(411)	90.885	24.124	8	23	0.83	0.64
(420)	93.284	26.565	4	7	0.80	0.58

(110) in Figure 4(b), occurs at a slightly lower angle than the expected inclination ($\psi = 45°$) due to defocusing effects. As for the top layer, the substrate layer does not show any in-plane preferred orientation. Lets now evaluate the corresponding TC value for a textured polycrystalline F:SnO_2 made of isotropic grains with a polar distribution characterized by a FWHM as the one observed, i.e., $\Delta\psi = 60°$. For simplicity, we take a Gaussian distribution of the form

$$f_{text} \propto \exp\left(-\ln(2)\left(\frac{2\psi}{\Delta\psi}\right)^2\right). \quad (4)$$

Following Eq. (1) and taking the correction values calculated trough Eq. (4) (last column of Table II) we obtain TC(200) = 2.8, almost the same value directly obtained from the observed intensities. This last result excludes definitively any morphologic contribution to the TC, confirming the grain isotropy of commercial F:SnO_2 polycrystalline films. In summary, using the average-like texture coefficient defined in expression (1) for the characterization of one-dimensional oriented nanostructures would induce serious overestimations of the texture.

As stated in the introduction, the standard powder diffractometer, available in almost any material research lab, is used to provide a rapid feedback when adjusting the growing parameters of the new nano-materials. The important question that arises at this point is: is it possible to obtain both, satisfactory texture and shape information, just from the BB diffraction spectra? Based on the above discussion, our answer is positive. To see how it works, it is enough to notice that these two ingredients (shape and texture) combine as a product to produce the actual correction in the relative intensities

$$f_{corr} = f_{shape} f_{text} = \max[\cos^2\psi, r^2\sin^2\psi]\exp\left(-\ln(2)\left(\frac{2\psi}{\Delta\psi}\right)^2\right). \quad (5)$$

Fitting the ratio I_{hkl}/I_{hkl}^0 for all available reflections in the BB XRD spectra with expression (5), one can find the two adjustable parameters: the aspect ratio r and the FWHM of the polar distribution. However, the method is based on three basic assumptions: (i) the direction of the texture coincides with the long axis of the crystallites, (ii) the polar distribution has a Gaussian shape, and (iii): ZnO nanorods are arranged on the surface within a single layer, i.e., nanorods do not pile up on top of others. The first assumption is reasonable since in most one dimensional oriented nanostructures, the texture is produced (or enhanced) by a natural selection mechanism in which the crystallites growing at lower inclination with respect to the surface normal inhibits the growing of those growing at larger angles.[2] The second assumption is an approximation that provides a rough quantitative estimate of the angular spread. Finally, the third assumption is justified by the fact that most of the nanorods/nanowires samples are being grown on the substrate surface satisfying the"non-piling-up" condition. In the last column of Table I, we list the observed global correction factors (scaled so that $f_{corr}(002) = 1$) to be fitted by expression (5).

A fit of the correction factors listed in the last column of Table I is shown in Figure 5. The best fit with Eq. (5) is obtained for an aspect ratio $r = 0.47 \approx 1{:}2$ and a FWHM $\Delta\psi \approx 125°$. In order to check the consistency of the above results, a pure-shape correction (Eq. (3)) was used to fit the data producing an aspect ratio $r = 0.22 \approx 1{:}5$, which seems larger than the estimate one can do from the TEM image in Figure 2. Finally, a pure-texture Gaussian fit (Eq. (4)) yields an angular distribution with a FWHM of 75°, in clear contradiction with the Psi-scan in Figure 3(a). While the aspect ratio $r = 1{:}2$ obtained with the combined approach (Eq. (5)) seems small, compared with 1:4, as one can guess from the SEM picture in Figure 2, the FWHM is almost the same as the one obtained from the Psi-scan in Figure 3. Thus, in contrast with the use of Eq. (1), our procedure is able to give a correct estimate of the texture. The limited efficiency in predicting the aspect ratio is presumably due to both, the experimental errors on the intensity at high inclination angles and to the assumed Gaussian polar distribution. Nevertheless, the procedure indicates the existence of a shape anisotropy by clearly producing $r < 1$. Indeed, the same procedure applied to the isotropic F:SnO_2 bottom layer (see Figure 6) yields $r = 0.999 \approx 1$ and a FWHM of 74°. This FWHM, as well as the kink at $\psi = 45°$ are clearly artifacts due to the cylindrical model. Turning back to the spherical model, we found $\Delta\psi = 59°$, which is in excellent agreement with the Psi-scan in Figure 4.

As a last consistency check for the approach, let us analyze the GID of Figure 1(b) (dark curve) within the present model. In the GID geometry, the diffraction wave-vector (aligned along the bisecting line of the incident and detected beams) is no longer normal to the sample surface. The effective inclination $\tilde{\psi}$ of a given crystallographic plane with respect to the diffraction wave-vector direction depends not

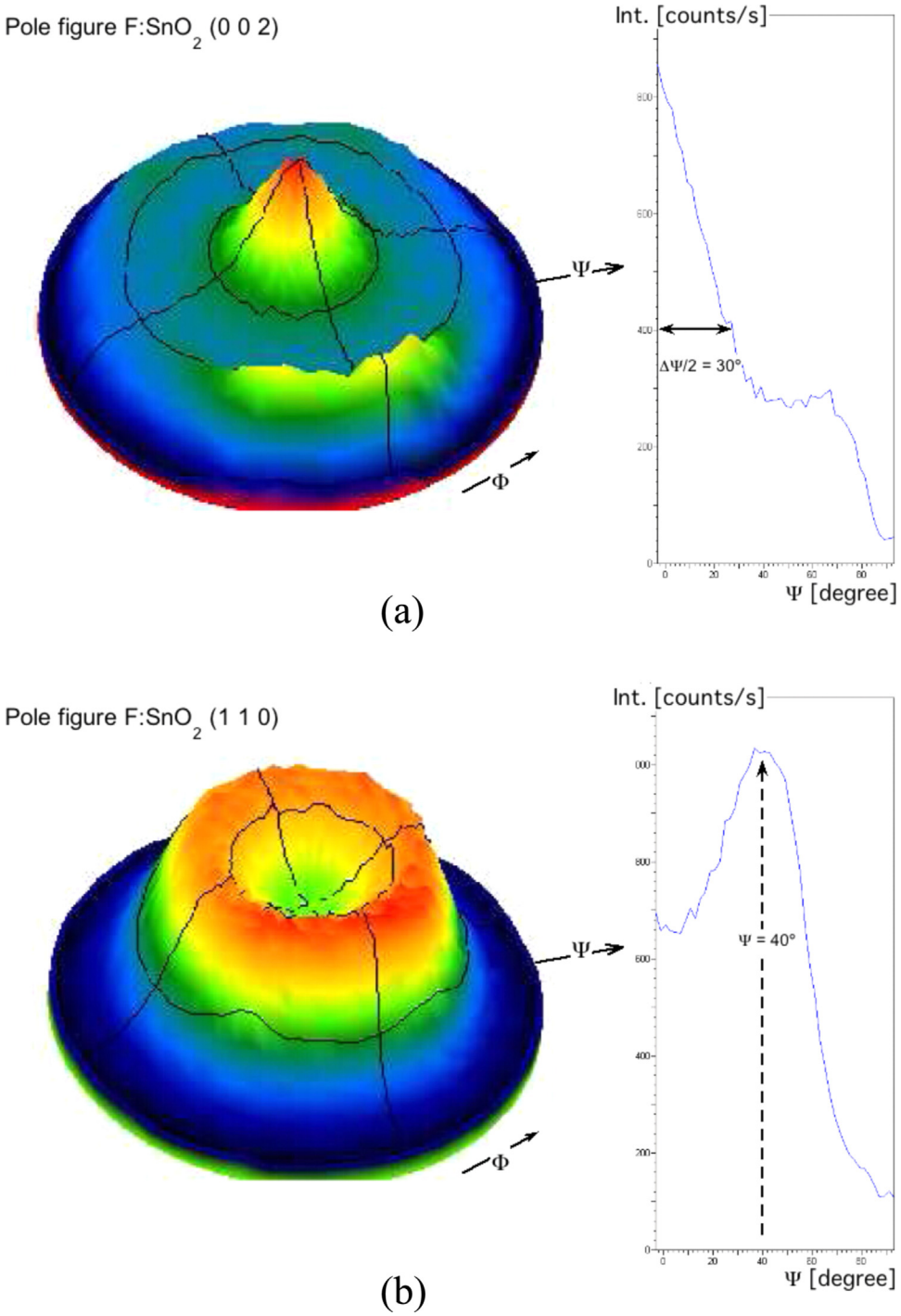

FIG. 4. (Color online) F:SnO $_2$ pole figures (200) in (a) and (110) in (b). 3D plot (left hand panel) and ψ scan (right hand panel).

only upon its inclination ψ with respect to the texture direction, but also on the Bragg angle θ, the fixed incident angle Ω and on its azimuthal direction ϕ. The correction factor of Eq. (5) is then generalized as follows:

$$f_{corr}^{GID} = \exp\left(-\ln(2)\left(\frac{2\psi}{\Delta\psi}\right)^2\right)\cdot\int_{-\pi}^{\pi}\frac{d\phi}{2\pi}[\cos^2(\tilde{\psi}(\theta)) + r^2\sin^2(\tilde{\psi}(\theta))], \tag{6}$$

where the integral on the azimuthal angle φ contains the ellipsoidal approximation of expression (3) which is easier to integrate. The expression for the effective inclination $\tilde{\psi}$ is

$$\tilde{\psi}(\phi) = \arccos(\cos(\psi)\cos(\alpha) - \sin(\psi)\sin(\alpha)\cos(\phi)); \quad \text{with } \alpha = \theta - \Omega. \tag{7}$$

Equation (6) admits an analytical integration and the final expression is

$$f_{corr}^{GID} = \exp\left(-\ln(2)\left(\frac{2\psi}{\Delta\psi}\right)^2\right)\cdot\left[r^2 + (1-r^2)(\cos^2(\psi)\cos^2(\alpha) + \frac{1}{2}\sin^2(\psi)\sin^2(\alpha))\right]. \tag{8}$$

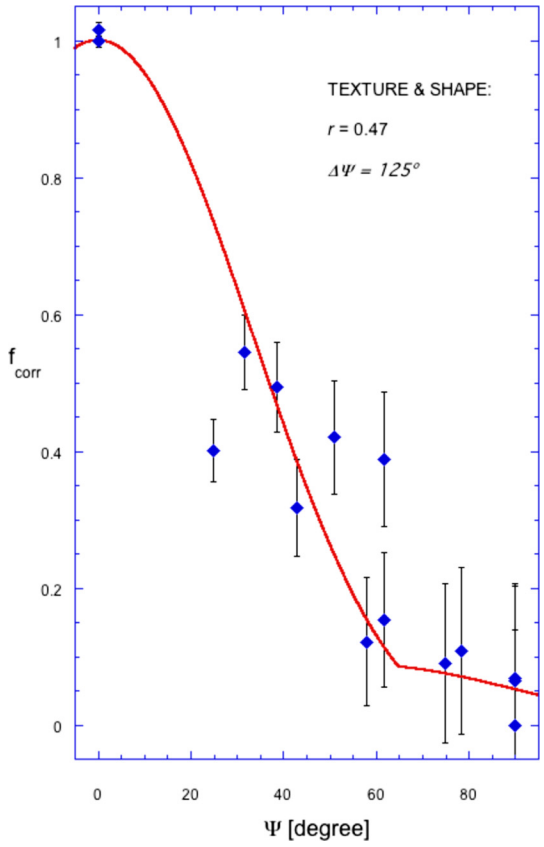

FIG. 5. (Color online) Fit of the observed intensity corrections on ZnO nano-rods using expression (5).

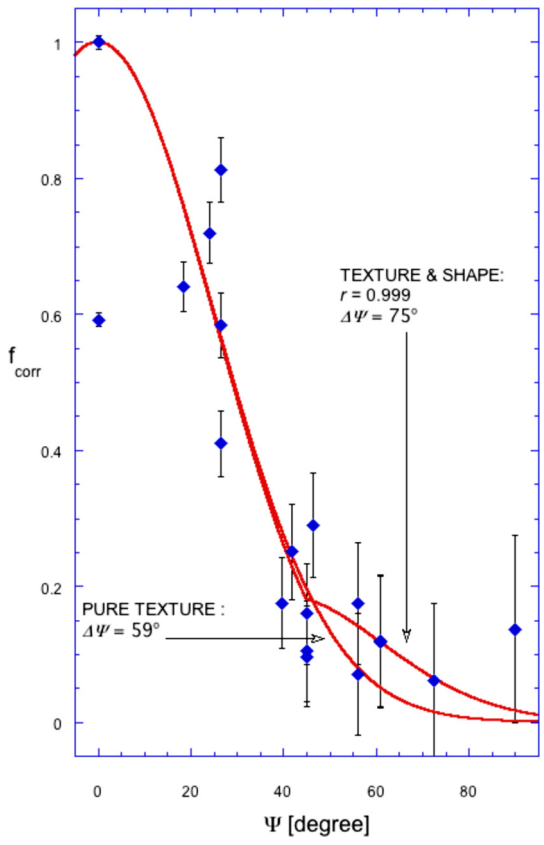

FIG. 6. (Color online) Comparative fits of the observed intensity corrections on the SnO_2 substrate film using expressions (4 and 5).

In contrast with Eq. (5), the GID correction factor (8) is a non-monotonous function of ψ, which depends on the particular crystallographic structure of the sample, through the parameter α. In Figure 7, we illustrate the trend of the GID correction factor (continuous line) given by Eq. (8), setting the value of the aspect ratio at $r = 0.47$, as extracted from the BB analysis, and adjusting manually the FWHM of the gaussian polar distribution to $\Delta\psi = 200°$. On the same graph, we also plot the pure shape correction ($r = 0.47$, $\Delta\psi = \infty$) and the pure texture correction ($r = 1.0$, $\Delta\psi = 200°$) for comparison. The experimental points are obtained from the ratio of the observed GID relative intensities and the roughly rounded powder intensities (from crystallographic tables). As a consequence, the error bars on the weakest peaks ($<10\%$) reach unreasonable values, and we therefore remove them from the graph. The trend in Figure 7 confirms again the importance of the morphology contribution to the relative XRD intensities and the correctness of the present approach.

As a summary, for the texture characterization of one-dimensional oriented nanostructures, we propose the following protocol:

(1) With a standard XRD powder diffraction setup, perform a $\theta - 2\theta$ scan (BB geometry) of the sample in the widest available angular range to obtain as much peaks as possible.
(2) Make a preliminary comparative inspection of the relative peak intensities to detect any substantial departure from the standard powder pattern:

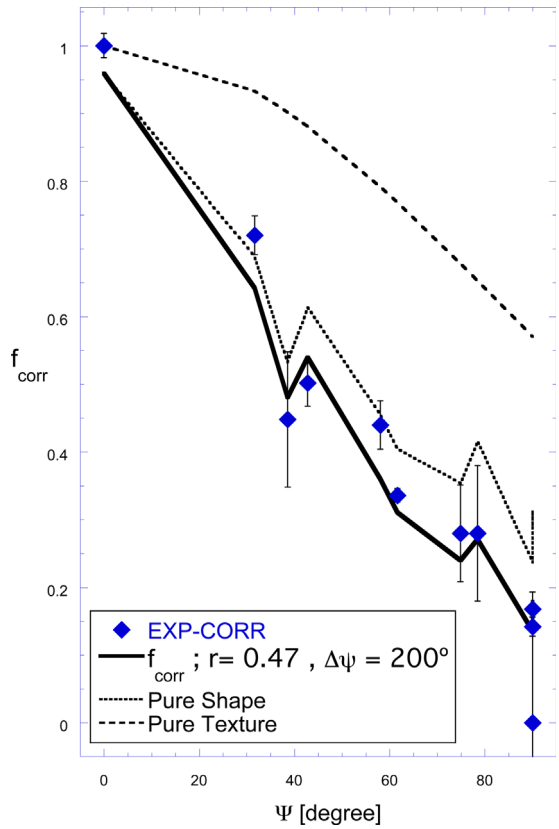

FIG. 7. (Color online) Observed GID intensity corrections (diamonds) on the ZnO nano-rods and comparison with the calculated correction (continuous line) using expression (8). The dashed line corresponds to the pure texture limit (r = 1.0), and the dotted line to the pure shape limit ($\Delta\psi = \infty$).

- Choose the most enhanced peak in your sample as a candidate for the texture.
- Optional: If the diffractometer allows decoupling between 2θ and θ (or Ω) axes, perform a GID under the same conditions to confirm the guessed texture: the guessed peak should be strongly reduced if intensity variations are dominated by the polar distribution; if not, you are dealing with anisotropic oriented crystallites.

(3) Report on a table, as a function of the inclination angle ψ_{hkl}, the intensity correction factors, scaled so that for the guessed texture diffraction planes -say (xyz)- one obtains $f_{corr}(xyz) = 1$. Fit $f(\psi)$ using Eq. (5) to extract the grain aspect ratio r and the FWHM $\Delta\psi$ of the Gaussian angular distribution.

IV. CONCLUSIONS

We have discussed the applicability of the usual texture coefficient method proposed by C. Barret and T. B. Massalski[10] in the context of texture characterization of one-dimensional oriented nanostructures. We found that for polycrystalline samples formed of a monolayer of highly anisotropic crystallites (nano-rods) with a given crystallographic orientation along their longer axis there is a strong contribution, beyond texture, of the crystallites shape on the relative Bragg peak intensities. This contribution results in a systematic overestimation of the sample texture. We then worked out an adapted method in order to include the grain morphology into the texture analysis. Our approach, as the one in Ref. 10, is based on the comparison between the observed relative diffraction intensities with those of a standard (isotropic) powder sample of the same compound. However, instead of using an average-like characteristic quantity such as the TC, we work with the correction factors as a function of the polar inclination of the crystallites. Our method allows discriminating between texture and morphology contributions, providing two characteristic parameters: the grain aspect ratio and the FWHM of the angular distribution. The main advantage of the method is that it only requires the use of a standard powder diffractometer. Any sample can then be characterized with a single scan, allowing a rapid feedback when trying to optimize the growing conditions of one-dimensional novel nanostructures.

ACKNOWLEDGMENTS

We acknowledge the support received from PEDECIBA Física, ANII (Agencia Nacional de Investigación e Innovación), and the CSIC (Comisión Sectorial de Investigación Científica) of the Universidad de la República, in Montevideo, Uruguay. We would like to especially thank the University of Neuchâtel (Switzerland) for their generous gift of the Philips PW1840 diffractometer equipped with the X'Pert MRD goniometer.

[1] L. Vayssieres, Adv. Mater. **15**, 464 (2003).
[2] J. B. Baxter, A. M. Walker, K. van Ommering, and E. S. Aydil, Nanotechnology **17**, S304 (2006).
[3] J. H. Yang, G. M. Liu, J. Lu, Y. F. Qiu, and S. H. Yang, Appl. Phys. Lett. **90**, 103109 (2007).
[4] H. H. Guo, J. Z. Zhou, and Z. H. Lin, Electrochem. Commun. **10**, 146 (2008).
[5] Y. Hames, Z. Alpaslan, A. Ksemen, S. E. San, and Y. Yerli, Sol. Energy, **84**, 426 (2010).
[6] H. D. Yu, Z. P. Zhang, M. Y. Han, X. T. Hao, and F. R. Zhu, J. Am. Chem. Soc. **127**, 2378 (2005).
[7] J. H. Park, P. Muralidharan, and D. K. Kim, Mater. Lett. **63**, 1019 (2009).
[8] E. A. Dalchiele, R. E. Marotti, A. Cortés, G. Riveros, H. Gómez, L. Martínez, R. Romero, D. Leinen, F. Martin, and J. R. Ramos-Barrado, Physica E **37**, 184 (2007).
[9] G. Riveros, H. Gómez, A. Cortés, R. E. Marotti, and E. A. Dalchiele, Appl. Phys. A **81**, 1724 (2005).
[10] C. Barret and T. B. Massalski, *Structure of Metals* (Pergamon, Oxford, 1980), p. 1923.
[11] G. B. Harris, Philos. Mag. **43**, 113 (1952).
[12] M. D. Vaudin, M. W. Rupich, M. Jowett, G. N. Riley, Jr., and J. F. Bingert, J. Mater. Res. **13**, 2910 (1998).
[13] Joint Committee on Powder Diffraction Standards, Powder diffraction files: PDF-01-075-0576 for ZnO and PDF-01-077-0488 for SnO2.
[14] B. D. Cullity and S. Rstock, *Elements of X-ray Diffraction* (Prentice-Hall, New Jersey, 2001).
[15] The apparent 4-fold symmetry in Figure 3(b) is due to the rectangular shape of the sample surface under the elongated X-ray beam illumination.